Detectability of Quantum Effects in Gravitational Waves Emitted by Binary Black Hole Mergers

LIGO SURF 2020: Interim Report 1

Zoë Haggard
Pomona College

Mentors: Alan J. Weinstein and Colm Talbot
LIGO Collaboration, Caltech

(Dated: July 8, 2020)

Gravitational wave detectors such as Advanced LIGO and Advanced Virgo provide a test of the theory of General relativity in the strong-field, highly dynamical regime, such as in compact binary coalescences. General Relativity, a purely classical theory, does not incorporate quantum mechanics. It is thought, however, that quantum mechanics must modify gravity; quantum uncertainty must manifest itself during the merger of two black hole horizons. These quantum mechanical effects could be observable in gravitational waves detected by LIGO as small perturbations in the signal waveform and higher harmonics, not explainable by current understandings of general relativity. We propose to study the *detectability* of such quantum mechanical effects from binary black hole mergers for future LIGO observations.

I. MOTIVATION

In his general theory of relativity (GR), Einstein predicts the existence of gravitational waves. Just as an accelerating charge produces electromagnetic radiation, an accelerating mass will create gravitational radiation, or, gravitational waves (GWs). GWs emit outwards at the speed of light, and, in the far-field, are described by a complex strain, $h = h_+ - ih_\times$, on space-time: the passing waves cause the distance between freely falling objects ('test masses') to oscillate at the frequency and amplitude of the GWs [1]. But gravitation, compared to electromagnetism, is much weaker. To observe gravitational radiation on Earth, highly massive and dynamic systems – such as coalescing compact binary black hole (BBH) systems – are needed in conjunction with large and precise detectors. In recent years, the Laser Interferometer Gravitational-Wave Observatory (LIGO) and Advanced Virgo have successfully observed GWs from compact binary mergers [2][3].

The coalescence of a BBH system is described by three major phases: inspiral, merger, and ringdown [4]. In the inspiral phase, the two black holes emit gravitational waves (roughly) proportional to their orbital frequencies; their orbital radius decreases with the GW emission. After the last stable orbit, the two horizons plunge into each other and merge during the merger phase. Finally, once the BHs' horizons come together, the system falls to equilibrium in the ringdown phase by emitting GWs at specific modes, called quasi-normal modes (QNMs). The QNMs can be calculated from black hole perturbation theory, which takes into account the final black hole's spin and mass [5].

Generally, the signals received at detectors are found to be dominantly quadrupolar [4]. For waveform creation and GWs analysis, the gravitational radiation assumed to be dominantly quadrupolar ($l = 2$, $m = 2$) for ease of analysis. This is usually a good assumption, as higher order modes tend to be negligible; their magnitudes are much smaller than the dominant quadrupole, making them hard to disentangle from the noise. With just the dominant quadrupolar multipole, intrinsic characteristics, such as the individual BH's mass and spin, and extrinsic characteristics, such as location, inclination (relative to the observer's line of sight), and the time of merger, can be inferred from the strain received at a network of detectors [6].

Recently, however, higher harmonics have been observed in compact binary mergers. GW190412 and GW190814, for instance, both show evidence of an octopole ($l = 3$, $m = 3$) mode [7][8]. This opens up a new domain for testing the predictions of GR at no-quadrupolar multipoles. The study of higher order modes – black hole spectroscopy – presents a way to look for deviations from GR.

At the event horizon of a black hole, for example, it is thought that GR should be modified by quantum mechanics or other unknown effects. Alternates to black holes exist, such as exotic compact objects (ECOs), but it is generally agreed that quantum uncertainty must become important past the horizon [9]. There, however, are very few concrete predictions of the observable effects QM would have on a black hole merger. Recent work done by Brustein *et al*, using a semi-classical perturbed black hole binary model, suggests that quantum emission would result in a higher emitted flux than predicted by GR, which, to an observer, could suggest a non-empty black hole interior [10]. As the BH horizon is deformed during the ringdown, the quantum emission creates additional quantum modes for both quadrupolar and higher orders [11]. Looking at these deviations, then, requires a multimodal analysis: understanding GR's non-quadrupolar predictions, so as not to mistake a higher, GR-mode, for a quantum ringdown mode.

Generally, the QNMs received at the detector can be written as a linear superposition of damped sinusoids,

$$h(t) = \sum_{j=1} A_j e^{2i\pi f_{o,j} t + i\phi_j} e^{-\frac{t}{\tau_j}} \quad (1)$$

where A_j is the amplitude of term j, $f_{o,j}$ is the central frequency of the particular mode, ϕ_j is the phase shift, and τ_j is the decay time, or the time required for the amplitude to drop by a factor of $1/e$ [7].

The Fourier transform, which shifts to the frequency domain, is a useful tool for signal analysis: it helps to pinpoint higher harmonics and easily analyze the other wave characteristics. The Fourier transform of a damped sinusoid is the Lorentzian [12]. Centered at f_o, the Lorentzian is written as,

$$\tilde{h}(f) = \sum_{j=1} A_j e^{i\phi_j} \frac{1}{2\pi} \frac{\gamma_j}{((f_j - f_{o,j})^2 + \frac{1}{2}{\gamma_j}^2)} \quad (2)$$

where $f_{o,j}$ is the frequency of the mode and $\gamma_j = \frac{1}{\tau_j}$.

The additional quantum ringdown modes in the time domain have similar form to Equation 1, but are composed of different frequencies, amplitudes, and time constants [11].

Putting the quantum ringdown with the GR QNM (Equation 1), a deviation from GR in the time domain, then, would be written as a small distortion in the GR variables – δA, $\delta\phi$, δf_o, and $\delta\tau$. This distortion can be written as,

$$h'(t) = \sum_{j=1} (A_j + \delta A_j) e^{2i\pi t (f_{o,j} + \delta f_{o,j})} e^{i(\phi_j + \delta\phi_j)} e^{-\frac{t}{\tau_j + \delta\tau_j}} \quad (3)$$

II. PROJECT & METHOD OVERVIEW

This project focuses on testing and employing these *ad hoc* deviations described by Brustein *et al* [10]. The main work of this project is to determine whether the quantum variations (see the Equation 3) in the GW are *significantly* detectable by the LIGO network at various signal-to-noise ratios (SNRs) and various BH binary masses.

First, without using quantum deviations, we will simulate a noiseless signal to fit for ringdown modes, verifying that we can recover them. Once this is completed, we will move onto looking at the quantum ringdown. Given a specific Kerr BH, we will simulate quantum deviations in waveforms, beginning at high SNR (e.g. 100 or more) and then moving to lower values. Using the python package `bilby`, we will infer the posterior distributions for the parameters describing the ringdown and quantify the significance at each SNR [13].

Understanding the influence of SNR on detection significance, we will move to the effect of mass ratio using the same analysis techniques as described above. Higher mass black hole binaries, for one, have a lower orbital frequency. Received gravitational wave frequency can approximately be written in terms of the orbital frequency as,

$$f \approx m f_s \quad (4)$$

where f is the frequency of a particular multipole, m, the magnetic number, is an integer, and f_s is the rotational frequency of the BH [7]. LIGO, operating between 20 Hz and 2000 Hz, may only see higher order modes if the mass of the BHs is within a specific range. Therefore, it is important to look at how BH mass influences detection and what kind of binary mergers can LIGO best uncover quantum distortions.

III. CURRENT WORK

A. Background Work

As background preparation, I worked through the GW analysis software using the open data workshop tutorials (tutorial Day 1 and tutorial Day 2). From the Day 1 tutorials, I learnt how to use the `gwosc` package for retrieving data and using the `TimeSeries` object in `gwpy` to transform data to the frequency domain (spectrogram, asd, q-transforms, and fft). Also from the Day 1 section I began to use the `pycbc` package. With this package, I was able to create time and frequency domain representations using different approximants; by the end of the tutorial, I was able to see how mass and distance affect the shape of the resultant waveform, specifically the ringdown.

From the Day 2 tutorials, I learnt how to use the Bayesian parameter estimation package, `bilby`, and the basics of matched filtering with `pycbc`. As I am new to Bayesian statistics and the logistics of sampling methods, I spent some time reading about Bayesian analysis, the `bilby` documentation, and the docs for `dynesty`, which is the preferred nested sampler used by `bilby` [14][15].

B. Simulated Signal Recovery

In `bilby`, I created a general damped-sinusoid model with both plus and cross polarization. The goal was to be sure I could recover my input parameters: amplitude h_o, frequency, and damping time (Figure 1). The main challenge of this was figuring out how to use inputs in `bilby` to speed up the `dynesty` sampling process [15].

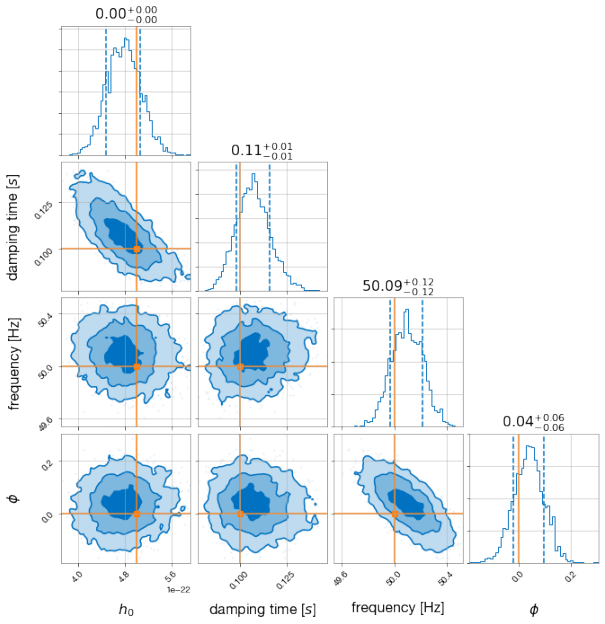

FIG. 1. Recovering input parameters (amplitude h_o, damping time, frequency, and phase) of single damped sinusoid in `bilby`. The original values of each parameter is marked by the orange lines.

Next, I moved on to create a model that could create a superposition of damped sinusoids (Equation 1). The goal of this task was to create a model of a Kerr BH ringdown for a specific a, dimensionless spin, and mass. In order to do this, I needed to learn how to use a package to recover QNM. At the beginning, I was experimenting with a package called `pyRing` for BH QNM, but I came across some debugging trouble using it on my computer, so I shifted to the package `qnm`, which recovers the complex-valued frequency for a given mode, (l, m, n) at a given a [16]. Understanding how to use the `qnm` package, I created a general model of superimposed damped-sinusoids. For simplicity's sake, I kept the amplitude and phase of the modes the same (though this is unphysical, as we would at least expect higher order modes to be smaller in amplitude). I tested the model in `bilby` by creating a superposition of the modes (2,2,0), (2,2,1), (2,2,2), (3,3,0) for $a = 0.5$ and $M = M_\odot$. I was able to recover the inputted phase, a, mass, and amplitude (Figure 2).

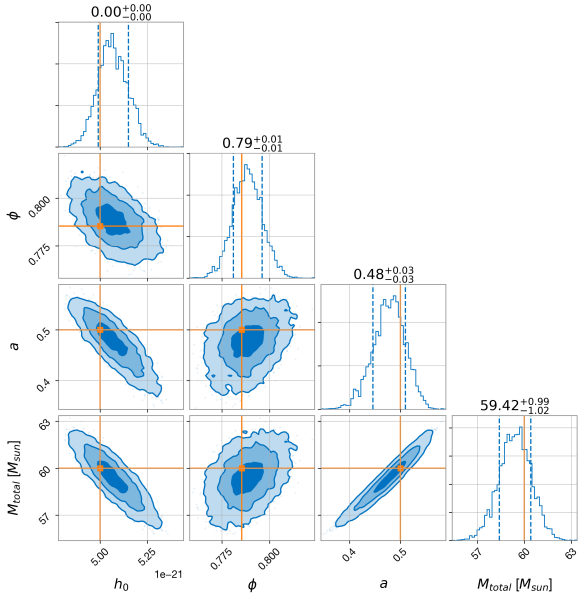

FIG. 2. Recovering input parameters in `bilby` using a superposition of damped sinusoids. The superposition is created from four Kerr QNM modes: (2,2,0), (2,2,1), (2,2,2), (3,3,0). Here the sampled parameters are amplitude h_o, M_{total} in units M , dimensionless spin a, and phase .

C. QNM Visualization & Waveform Optimization

I visualized the effects that different parameters (inclination, mass-ratio q, distance) have on the ringdown for three different models which incorporate higher order modes: NRSur7dq4, SEOBNRv4PHM, and IMRPhenomPv3HM (Figure 3). From this, I saw that NRSur7dq4 (navy) and SEOBNRv4PHM (cyan) have a similar shape, although off by a small phase shift and slightly different in amplitude, at least by eye. IMRPhenomPv3HM (red) appears the most different, off by around a complete phase.

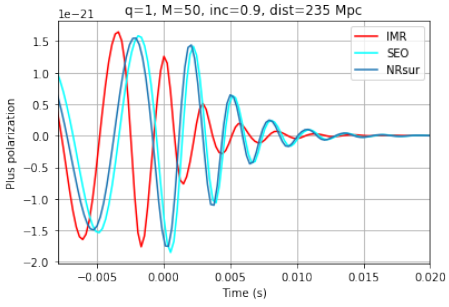

FIG. 3. Ringdown for 3 different models which include higher order modes: NRSur7dq4 (navy), SEOBNRv4PHM (cyan), and IMRPhenomPv3HM (red). Calculated with $M = 50M$, $q = 1$, $inclination = 0.9$, and $distance = 235Mpc$.

After looking at the differences in the models, I shifted to looking at NRSur7dq4 in particular, which is able to

easily plot modes separately. I saw that $m \neq l$ modes have a lower frequency compared to the dominant (2, 2) mode, and are lower in amplitude, which is as I expected (Figure 4).

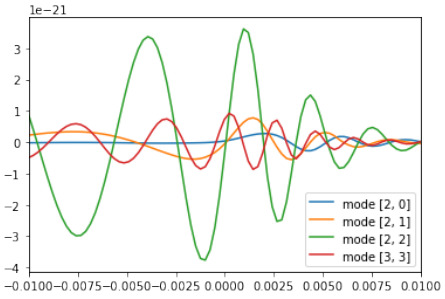

FIG. 4. NRSur7dq4 model: plot of different modes to visualize the relative change of amplitude and frequency. The x-axis represents time (in seconds) and the y-axis is amplitude.

Next, I worked on seeing if I could recover the expected QNM frequency for a single mode using a damped-sinusoid curve fit (with NRSur7dq4). I chose to work with the (2,2,0) mode, with $M = 44$ and $a = 0$. From the `qnm` package, this mode should have a frequency of 287 Hz and a decay time of 0.003 seconds. Using `scipy.optimize.curve_fit`, I found that the fit gave me results within the order of the expected QNM: a frequency around 300 Hz and a decay time around 0.003 seconds (Figure 5).

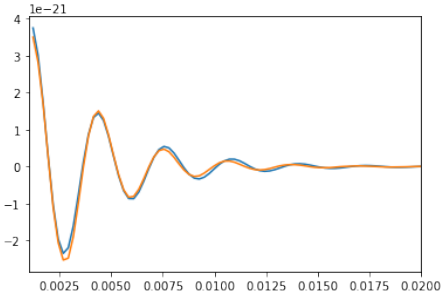

FIG. 5. Fit of NRSur7dq4 model for (2,2,0) mode and $M = 44$, $a = 0$. Here, blue is the original model and orange is the fit. The x-axis represents time (in seconds) and the y-axis is amplitude.

D. Quantum Ringdown Model

Following Ram Brustein and Yagi, I used a model for a non-GR ringdown that assumes a collapsed polymer [11]. In this model, the ringdown is similar to Equation 1, but with a start time shift, t_j,

$$h'(t) = \sum_{j=1} A'_j e^{2i\pi f'_{o,j}(t-t_j)+i\phi'_j} e^{-\frac{t-t_j}{\tau'_j}} \tag{5}$$

where the other parameters as the same as defined above in Equation 1. The ringdown angular frequencies are written as,

$$\omega_p = \frac{p\pi}{2R_s n_{ref}} - i\frac{1}{R_s n_{ref}^2} \tag{6}$$

where p is an odd integer, R_s is equivalent to the r_+ Kerr solution, and n_{ref} is the refractive index of the quantum material inside the BH. In the case of this model, they find n_{ref} to be inversely proportional to g_s, the coupling constant for quantum strings [11]. Using this setup, I visualized the difference between this model, and the model predicted by GR. For instance, varying mass, we see that the start time (t_j) is delayed further with increasing mass and the frequency decreases (Figure 6). Furthermore, when compared to GR QNM, the predicted QNM are much lower in frequency.

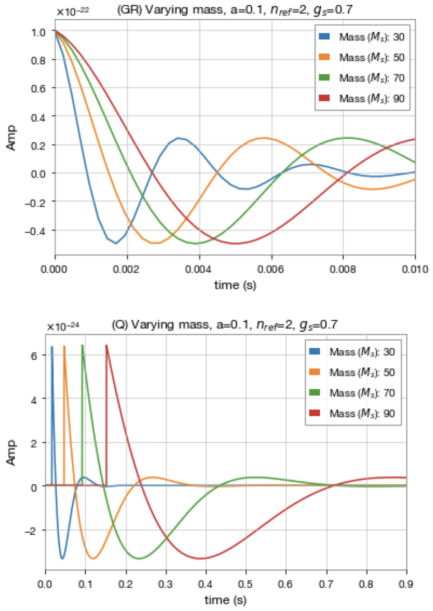

FIG. 6. Varying mass using Ram Brustein and Yagi model for $a = 0.1$, $n_{ref} = 2$, and $g_s = 0.7$. The GR predictions (which do not depend on g_s or n_{ref}, only a and $mass$) are in the top graph, while the Quantum predictions are in the bottom graph.

IV. CHALLENGES & MOVING FORWARD

Moving forward, I will be working on further understanding the model created by Ram Brustein and Yagi, especially working towards a better understanding of the parameters. A challenge I am currently having with it is that its predicted frequencies are very low, smaller than 30 Hz when the mass is larger than 20 M_{sun} (Figure 7). This may be an error in the code I wrote, or a misunderstanding of the model, so more work and reading may help clarify this.

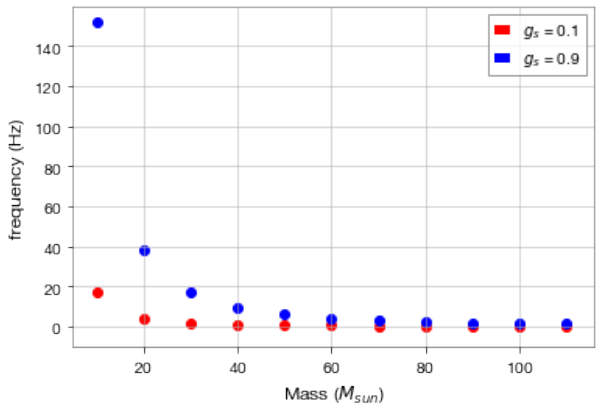

FIG. 7. Plot of mass (M) versus real frequency (Hz) for two different g_s, 0.1 in red and 0.9 in blue

Another thing I will be working on is creating a general model as described in Equation 3, using GR QNM and setting the quantum deviations as free parameters. I already know I can recover regular Kerr QNM with `bilby` (Figure 2), so it is only a matter of adding the general deviations into the function definition. With this model, then, I will insert random parameters and see if they can be recovered by `bilby`, first at no noise, then with noise (different levels of SNR). As a preliminary step, it may be helpful to work with a single added quantum mode, then add more. A challenge I can foresee is figuring out a good choice for amplitude of the GR modes and added quantum modes. One possibility is that I could set the amplitude for the GR modes, and then make the quantum modes some fraction of the GR mode's amplitude.

A general challenge I have been having over the past few weeks is also keeping organized files, directories, and python notebooks. Also, I now realize that it is important to label axes on figures, even in notebooks: it is hard add labels after the figure is created. Moving forward, I want to work towards a more organized workplace for my documents, and writing a key for my file organization that I can refer back to.

[1] T. Moore, *A General Relativity Workbook* (University Science Books, 2012).
[2] L. S. Collaboration and *et al*, Advanced ligo, arXiv (2015).
[3] F. Acernese and *et al*, Advanced virgo: a second-generation interferometric gravitational wave detector, arXiv (2015).
[4] B. P. Abbott and *et al*, Observation of gravitation waves from a binary black hole merger, Phys. Rev. Letters **116** (2016).
[5] V. C. Emanuele Berti and A. O. Starinets, Quasinormal modes of black holes and black branes, arXiv (2009).
[6] B. P. Abbott and *et al*, Gwtc-1: A gravitational-wave transient catalog of compact binary mergers observed by ligo and virgo, Phys. Rev.X **9** (2019).
[7] LIGO and VIRGO, Gw190412: Observation of a binary-black-hole coalescence with asymmetric masses, arXiv (2020).
[8] R. Abbott and *et al*, Gw190814: Gravitational waves from the coalescence of a 23 solar mass black hole with a 2.6 solar mass compact object, arXiv (2020).
[9] R. Brustein and A. Medved, Non-singular black holes interiors need physics beyond the standard model, Progress of Physics **67** (2019).
[10] R. Brustein and Y. Sherf, Emission channels from perturbed quantum black holes, Phys. Rev. D **100** (2019).
[11] A. M. Ram Brustein and K. Yagi, When black holes collide: Probing the interior composition by the spectrum of ringdown modes and emitted gravitational waves, arXiv (2017).
[12] Lorentzian function: Wolfram mathworld, `https://mathworld.wolfram.com/LorentzianFunction.html`.
[13] Bilby documentation, `https://lscsoft.docs.ligo.org/bilby/index.html`.
[14] G. Ashton and *et al*, Bilby: A user-friendly bayesian inference library for gravitational-wave astronomy, arXiv (2018).
[15] Dynamic nested sampling with dynesty, `https://dynesty.readthedocs.io/en/latest/dynamic.html`.
[16] `qnm` documentation, `https://qnm.readthedocs.io/en/latest/`.